A Higher-Order Unstructured Finite Volume Solver for Three-Dimensional Compressible Flows

Shayan Hoshyari
Supervisor: Dr. Carl Ollivier-Gooch

University of British Columbia

August, 2017

Computational Fluid Dynamics — Application

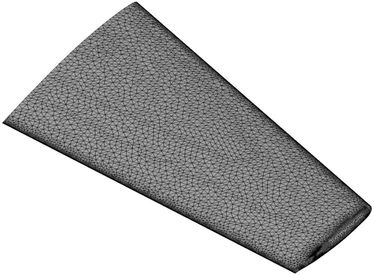

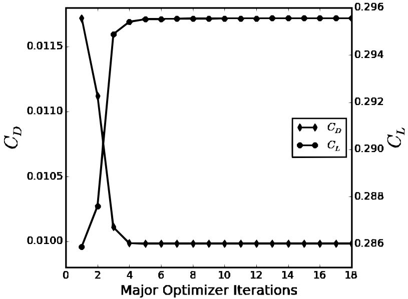

Optimal shape design of an Onera M6 wing (SU2)

Higher-Order Accurate Methods

- Conventional methods are second-order accurate $\|u - u_h\| = O(h^2)$

Higher-Order Accurate Methods

- Conventional methods are second-order accurate $\|u - u_h\| = O(h^2)$
- Higher-order methods can reduce computational costs

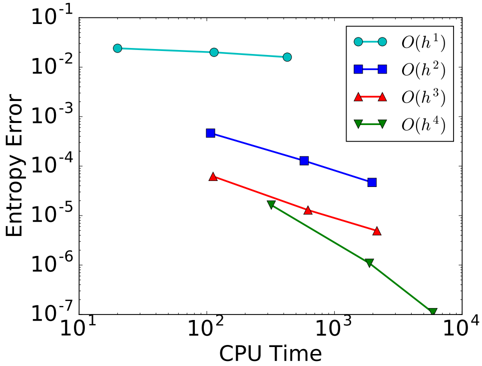

Inviscid flow around a sphere

Higher-Order Accurate Methods

- Conventional methods are second-order accurate $\|u - u_h\| = O(h^2)$
- Higher-order methods can reduce computational costs
- Unstructured finite volume methods

Higher-Order Accurate Methods

- Conventional methods are second-order accurate $\|u - u_h\| = O(h^2)$
- Higher-order methods can reduce computational costs
- Unstructured finite volume methods
  - Complex geometries

Higher-Order Accurate Methods

- Conventional methods are second-order accurate $\|u - u_h\| = O(h^2)$
- Higher-order methods can reduce computational costs
- Unstructured finite volume methods
  - Complex geometries
  - Easier integration into FV commercial solvers

Higher-Order Accurate Methods

- Conventional methods are second-order accurate $\|u - u_h\| = O(h^2)$
- Higher-order methods can reduce computational costs
- Unstructured finite volume methods
  - Complex geometries
  - Easier integration into FV commercial solvers
  - Smaller number of DOF compared to FEM

Higher-Order Accurate Methods

- Conventional methods are second-order accurate $\|u - u_h\| = O(h^2)$
- Higher-order methods can reduce computational costs
- Unstructured finite volume methods
  - Complex geometries
  - Easier integration into FV commercial solvers
  - Smaller number of DOF compared to FEM
- Previous work:

Higher-Order Accurate Methods

- Conventional methods are second-order accurate $\|u - u_h\| = O(h^2)$
- Higher-order methods can reduce computational costs
- Unstructured finite volume methods
  - Complex geometries
  - Easier integration into FV commercial solvers
  - Smaller number of DOF compared to FEM
- Previous work:
  - Inviscid flow (Haider et al., 2014; Michalak and Ollivier-Gooch, 2009)

Higher-Order Accurate Methods

- Conventional methods are second-order accurate $\|u - u_h\| = O(h^2)$
- Higher-order methods can reduce computational costs
- Unstructured finite volume methods
  - Complex geometries
  - Easier integration into FV commercial solvers
  - Smaller number of DOF compared to FEM
- Previous work:
  - Inviscid flow (Haider et al., 2014; Michalak and Ollivier-Gooch, 2009)
  - Laminar flow (Li, 2014; Haider et al., 2009)

Higher-Order Accurate Methods

- Conventional methods are second-order accurate $\|u - u_h\| = O(h^2)$
- Higher-order methods can reduce computational costs
- Unstructured finite volume methods
  - Complex geometries
  - Easier integration into FV commercial solvers
  - Smaller number of DOF compared to FEM
- Previous work:
  - Inviscid flow (Haider et al., 2014; Michalak and Ollivier-Gooch, 2009)
  - Laminar flow (Li, 2014; Haider et al., 2009)
  - 2-D turbulent flow (Jalali and Ollivier-Gooch, 2017)

Higher-Order Accurate Methods

- Conventional methods are second-order accurate $\|u - u_h\| = O(h^2)$
- Higher-order methods can reduce computational costs
- Unstructured finite volume methods
    - Complex geometries
    - Easier integration into FV commercial solvers
    - Smaller number of DOF compared to FEM
- Previous work:
    - Inviscid flow (Haider et al., 2014; Michalak and Ollivier-Gooch, 2009)
    - Laminar flow (Li, 2014; Haider et al., 2009)
    - 2-D turbulent flow (Jalali and Ollivier-Gooch, 2017)
    - 3-D turbulent flow

Higher-Order Accurate Methods

- Conventional methods are second-order accurate $\|u - u_h\| = O(h^2)$
- Higher-order methods can reduce computational costs
- Unstructured finite volume methods
  - Complex geometries
  - Easier integration into FV commercial solvers
  - Smaller number of DOF compared to FEM
- Previous work:
  - Inviscid flow (Haider et al., 2014; Michalak and Ollivier-Gooch, 2009)
  - Laminar flow (Li, 2014; Haider et al., 2009)
  - 2-D turbulent flow (Jalali and Ollivier-Gooch, 2017)
  - 3-D turbulent flow
- Long term goal at ANSLab:
  3-D higher-order finite volume flow solver for all flow conditions

Objective

Goal: solution of 3-D inviscid and viscous turbulent benchmark flow problems

Objective

Goal: solution of 3-D inviscid and viscous turbulent benchmark flow problems

- 3-D finite volume formulation for
  Reynolds Averaged Navier-Stokes + Spalart-Allmaras turbulence model

Objective

Goal: solution of 3-D inviscid and viscous turbulent benchmark flow problems

- 3-D finite volume formulation for
  Reynolds Averaged Navier-Stokes + Spalart-Allmaras turbulence model
- Implementing the mesh preprocessing steps in 3-D (mesh curving)

Objective

Goal: solution of 3-D inviscid and viscous turbulent benchmark flow problems

- 3-D finite volume formulation for
  Reynolds Averaged Navier-Stokes + Spalart-Allmaras turbulence model
- Implementing the mesh preprocessing steps in 3-D (mesh curving)
- Solution of the discretized system of nonlinear equations

Objective

Goal: solution of 3-D inviscid and viscous turbulent benchmark flow problems

- 3-D finite volume formulation for
  Reynolds Averaged Navier-Stokes + Spalart-Allmaras turbulence model
- Implementing the mesh preprocessing steps in 3-D (mesh curving)
- Solution of the discretized system of nonlinear equations
- Verification of performance and accuracy

Finite Volume Method

- Given a set of control volumes $\mathcal{T}_h$

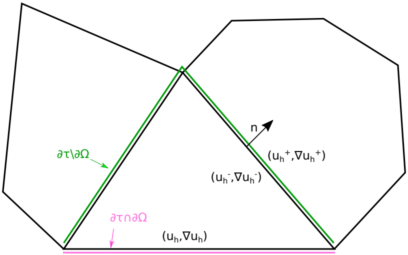

Finite Volume Method

- Given a set of control volumes $\mathcal{T}_h$
- Find $\mathbf{u}_h(\mathbf{x}; \mathbf{U}_h)$

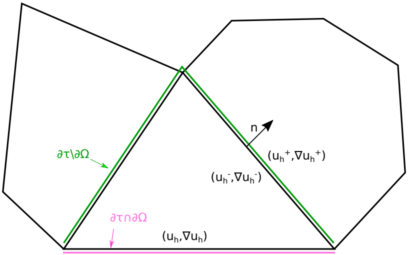

Finite Volume Method

- Given a set of control volumes $\mathcal{T}_h$
- Find $\mathbf{u}_h(\mathbf{x}; \mathbf{U}_h)$
- $\mathbf{U}_h \equiv$ DOF vector $\equiv$ control volume average values

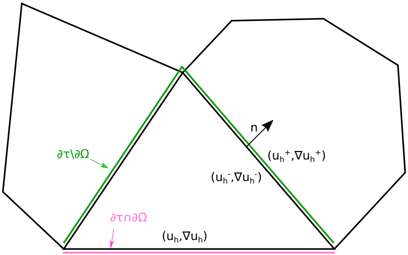

Finite Volume Method

- Given a set of control volumes $\mathcal{T}_h$
- Find $\mathbf{u}_h(\mathbf{x};\mathbf{U}_h)$
- $\mathbf{U}_h \equiv$ DOF vector $\equiv$ control volume average values
- Equations must be in the conservative form:
  $\frac{\partial \mathbf{u}}{\partial t} + \nabla \cdot (\boldsymbol{F}(\mathbf{u}) - \boldsymbol{Q}(\mathbf{u}, \nabla \mathbf{u})) = \mathbf{S}(\mathbf{u}, \nabla \mathbf{u})$

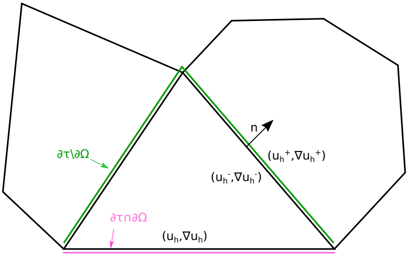

Finite Volume Method

Using the divergence theorem

$$\frac{d\mathbf{U}_{h,\tau}}{dt} + \frac{1}{\Omega_\tau}\int_{\partial\tau}\Big(\mathcal{F}(\mathbf{u}_h^+,\mathbf{u}_h^-) - \mathcal{Q}(\mathbf{u}_h^+,\nabla\mathbf{u}_h^+,\mathbf{u}_h^-,\nabla\mathbf{u}_h^-)\Big)\,dS - \frac{1}{\Omega_\tau}\int_\tau \mathbf{S}(\mathbf{u}_h,\nabla\mathbf{u}_h)\,d\Omega = 0$$

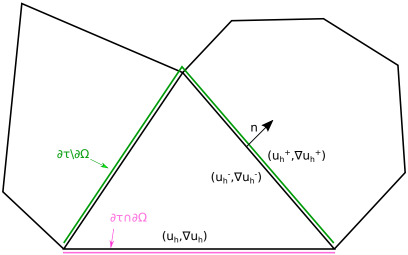

Finite Volume Method

Discretized system of equations

$$\frac{d\mathbf{U}_h}{dt} + \mathbf{R}(\mathbf{U}_h) = 0$$

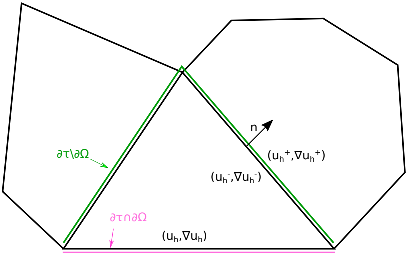

Finite Volume Method

Discretized system of equations

$$\frac{d\mathbf{U}_h}{dt} + \mathbf{R}(\mathbf{U}_h) = 0$$

Building blocks

- K-exact reconstruction: Defining $\mathbf{u}_h$ in terms of $\mathbf{U}_h$
- Numerical fluxes $\mathcal{F}$ and $\mathcal{Q}$

RANS + Negative S-A Equations

$$\mathbf{u} = \begin{bmatrix} \rho \\ \rho\mathbf{v} \\ E \\ \rho\tilde{\nu} \end{bmatrix} \quad \boldsymbol{F} = \begin{bmatrix} \rho\mathbf{v}^T \\ \rho\mathbf{v}\mathbf{v}^T + P\boldsymbol{I} \\ (E+P)\mathbf{v}^T \\ \tilde{\nu}\rho\mathbf{v}^T \end{bmatrix} \quad \boldsymbol{Q} = \begin{bmatrix} 0 \\ \boldsymbol{\tau} \\ (E+P)\boldsymbol{\tau}\mathbf{v} + \frac{R\gamma}{\gamma-1}\left(\frac{\mu}{Pr} + \frac{\mu_T}{Pr_T}\right)\nabla T \\ -\frac{1}{\sigma}(\mu+\mu_T)\nabla\tilde{\nu} \end{bmatrix}$$

$$\mathbf{S} = \begin{bmatrix} 0 \\ 0 \\ 0 \\ Diff + \rho(Prod - Dest + Trip) \end{bmatrix}$$

Euler	Laminar Navier-Stokes	RANS + S-A

K-exact reconstruction

Average values $\mathbf{U}_h \quad \longrightarrow \quad$ piecewise continuous $\mathbf{u}_h(\mathbf{x})$

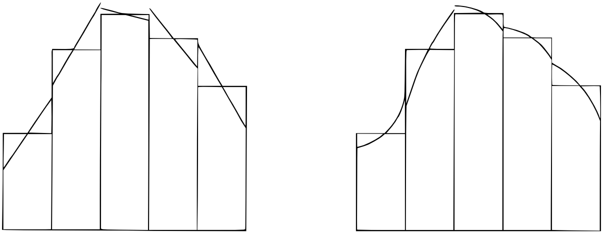

$k = 1$ $\qquad$ $k = 2$

K-exact reconstruction — Continued

For every control volume τ:

$$u_h(\mathbf{x};\mathbf{U}_h)|_{x\in\tau} = u_{h,\tau}(\mathbf{x};\mathbf{U}_h) = \sum_{i=1}^{N_{\mathrm{rec}}} a_\tau^i(\mathbf{U}_h)\phi_\tau^i(\mathbf{x}),$$

where

$$\left\{\phi_\tau^i(\mathbf{x})|i = 1\ldots N_{\mathrm{rec}}\right\} = \left\{\frac{1}{a!b!c!}(x_1 - x_{\tau 1})^a(x_2 - x_{\tau 2})^b(x_3 - x_{\tau 3})^c|a+b+c \le k\right\}.$$

K-exact reconstruction — Continued

- Select a specific set of each control volume's neighbors as its reconstruction stencil $Stencil(\tau)$
- $|Stencil(\tau)| \geq MinNeigh(k) \approx 1.5 N_{\text{rec}}(k)$

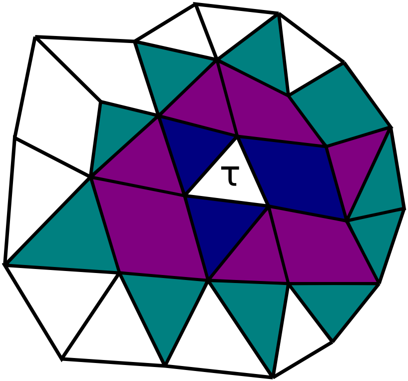

$k = 1$
$k = 2$
$k = 3$

K-exact reconstruction — Continued

- Predict the average values of $Stencil(\tau)$ members closely
- Satisfy conservation of the mean

$$\underset{a_\tau^1 \ldots a_\tau^{N_{\text{rec}}}}{\text{minimize}} \quad \sum_{\sigma \in Stencil(\tau)} \left(\frac{1}{\Omega_\sigma} \int_\sigma u_{h,\tau}(\mathbf{x}) d\Omega - U_{h,\sigma} \right)^2$$

$$\text{subject to} \quad \frac{1}{\Omega_\tau} \int_\tau u_h(\mathbf{x}) d\Omega = U_{h,\tau}$$

Numerical Flux Functions

Inviscid flux — Roe's flux function

$\mathcal{F}(\mathbf{u}_h^+, \mathbf{u}_h^-)$ = approximate flux in

$$\frac{\partial \mathbf{u}}{\partial t} + \frac{\partial \boldsymbol{F}(\mathbf{u})\mathbf{n}}{\partial s} = 0$$

Viscous flux — averaging with damping

$\mathcal{Q}(\mathbf{u}_h^+, \nabla \mathbf{u}_h^+, \mathbf{u}_h^-, \nabla \mathbf{u}_h^-) = \boldsymbol{Q}(\mathbf{u}_h^*, \nabla \mathbf{u}_h^*)\mathbf{n}$

where $\mathbf{u}_h^* = \frac{1}{2}\left(\mathbf{u}_h^+ + \mathbf{u}_h^-\right)$

and $\nabla \mathbf{u}_h^* = \frac{1}{2}\left(\nabla \mathbf{u}_h^+ + \nabla \mathbf{u}_h^-\right) + \eta \left(\frac{\mathbf{u}_h^+ - \mathbf{u}_h^-}{\|\mathbf{x}_{\tau+} - \mathbf{x}_{\tau-}\|_2}\right)\mathbf{n}$

Mesh Curving

- Mesh boundary must match the actual geometry

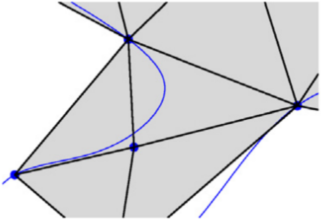

Mesh Curving

- Mesh boundary must match the actual geometry
- **No mesh tangling**

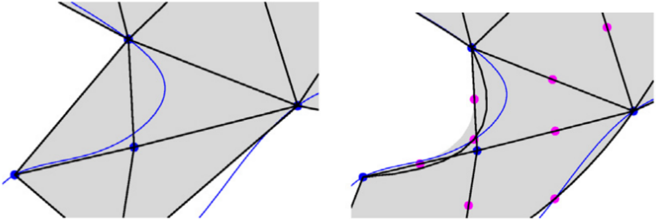

Mesh Curving

- Mesh boundary must match the actual geometry
- **No mesh tangling**
- FEM elasticity solver for displacing internal mesh faces (LibMesh)

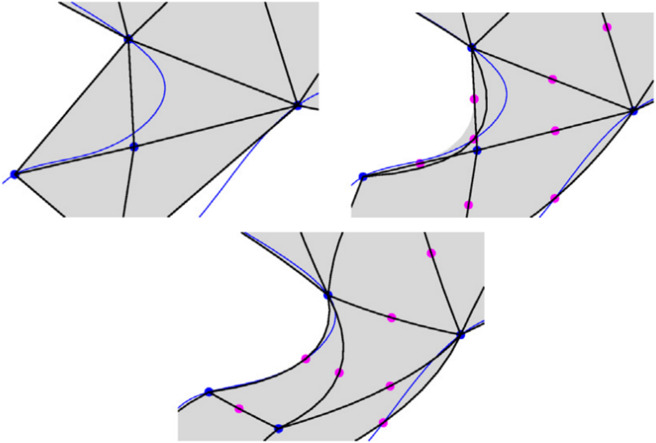

Mesh Curving – Continued

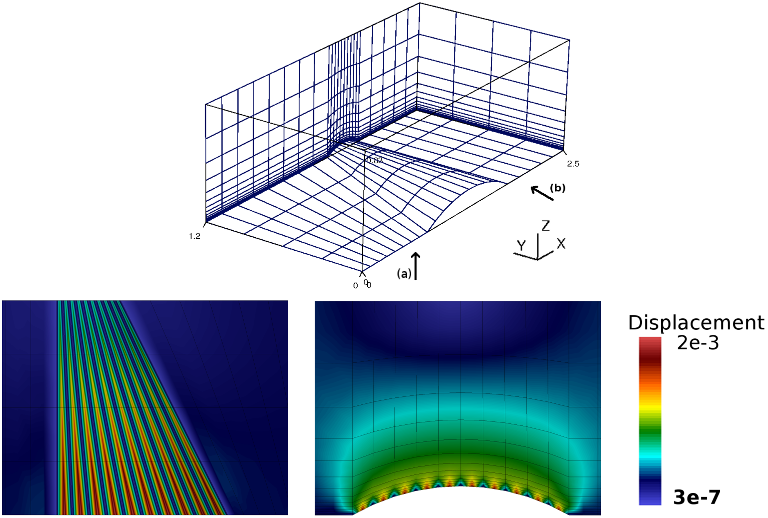

(a) (b)

Solution Scheme — PTC

- Seeking the steady state solution of:

$$\frac{d\mathbf{U}_h}{dt} + \mathbf{R}(\mathbf{U}_h) = 0$$

Solution Scheme — PTC

- Seeking the steady state solution of:

$$\frac{d\mathbf{U}_h}{dt} + \mathbf{R}(\mathbf{U}_h) = 0$$

- Pseudo transient continuation:

$$\left(\frac{\boldsymbol{V}}{\Delta t} + \frac{\partial \mathbf{R}}{\partial \mathbf{U}_h}\right) \delta\mathbf{U}_h = -\mathbf{R}(\mathbf{U}_h)$$

Solution Scheme — PTC

- Seeking the steady state solution of:

$$\frac{d\mathbf{U}_h}{dt} + \mathbf{R}(\mathbf{U}_h) = 0$$

- Pseudo transient continuation:

$$\left(\frac{\boldsymbol{V}}{\Delta t} + \frac{\partial \mathbf{R}}{\partial \mathbf{U}_h}\right) \delta \mathbf{U}_h = -\mathbf{R}(\mathbf{U}_h)$$

- A linear system must be solved:

$$\boldsymbol{A}\mathbf{x} = \mathbf{b}$$

Solution Scheme — GMRES

- Generalized minimal residual method (GMRES)

Solution Scheme — GMRES

- Generalized minimal residual method (GMRES)
  - Finds $\mathbf{x}^{(k)} \in \mathrm{Span}\{\mathbf{b}, \boldsymbol{A}\mathbf{b}, \boldsymbol{A}^2\mathbf{b}, \cdots, \boldsymbol{A}^{k-1}\mathbf{b}\}$

Solution Scheme — GMRES

- Generalized minimal residual method (GMRES)
  - Finds $\mathbf{x}^{(k)} \in \text{Span}\{\mathbf{b}, A\mathbf{b}, A^2\mathbf{b}, \cdots, A^{k-1}\mathbf{b}\}$
  - That minimizes $\|A\mathbf{x}^{(k)} - \mathbf{b}\|_2$

Solution Scheme — GMRES

- Generalized minimal residual method (GMRES)
  - Finds $\mathbf{x}^{(k)} \in \text{Span}\{\mathbf{b}, \boldsymbol{A}\mathbf{b}, \boldsymbol{A}^2\mathbf{b}, \cdots, \boldsymbol{A}^{k-1}\mathbf{b}\}$
  - That minimizes $\|\boldsymbol{A}\mathbf{x}^{(k)} - \mathbf{b}\|_2$

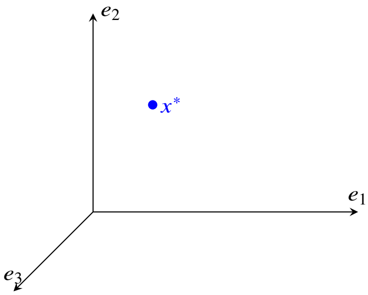

Solution Scheme — GMRES

- Generalized minimal residual method (GMRES)
  - Finds $\mathbf{x}^{(k)} \in \text{Span}\{\mathbf{b}, A\mathbf{b}, A^2\mathbf{b}, \cdots, A^{k-1}\mathbf{b}\}$
  - That minimizes $\|A\mathbf{x}^{(k)} - \mathbf{b}\|_2$

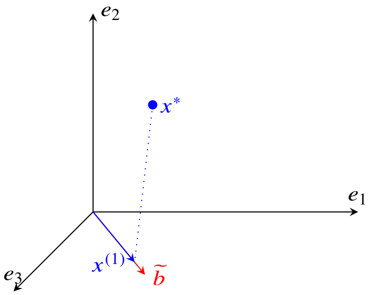

Solution Scheme — GMRES

- Generalized minimal residual method (GMRES)
  - Finds $\mathbf{x}^{(k)} \in \mathrm{Span}\{\mathbf{b}, \boldsymbol{A}\mathbf{b}, \boldsymbol{A}^2\mathbf{b}, \cdots, \boldsymbol{A}^{k-1}\mathbf{b}\}$
  - That minimizes $\|\boldsymbol{A}\mathbf{x}^{(k)} - \mathbf{b}\|_2$

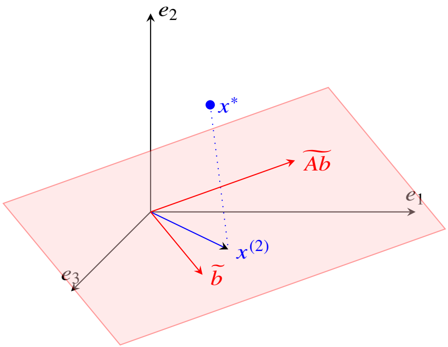

Solution Scheme — GMRES

- Generalized minimal residual method (GMRES)
  - Finds $\mathbf{x}^{(k)} \in \text{Span}\{\mathbf{b}, \boldsymbol{A}\mathbf{b}, \boldsymbol{A}^2\mathbf{b}, \cdots, \boldsymbol{A}^{k-1}\mathbf{b}\}$
  - That minimizes $\|\boldsymbol{A}\mathbf{x}^{(k)} - \mathbf{b}\|_2$

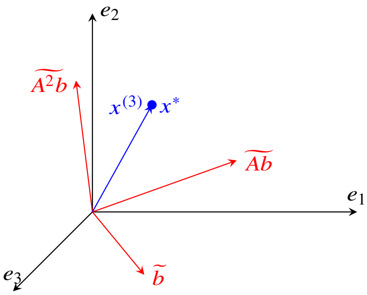

Solution Scheme — GMRES

- Generalized minimal residual method (GMRES)
  - Finds $\mathbf{x}^{(k)} \in \text{Span}\{\mathbf{b}, \boldsymbol{A}\mathbf{b}, \boldsymbol{A}^2\mathbf{b}, \cdots, \boldsymbol{A}^{k-1}\mathbf{b}\}$
  - That minimizes $\|\boldsymbol{A}\mathbf{x}^{(k)} - \mathbf{b}\|_2$
- Preconditioning $\quad \boldsymbol{A}\boldsymbol{P}\mathbf{y} = \mathbf{b}, \quad \mathbf{x} = \boldsymbol{P}\mathbf{y}$

Solution Scheme — GMRES

- Generalized minimal residual method (GMRES)
  - Finds $\mathbf{x}^{(k)} \in \mathrm{Span}\{\mathbf{b}, \boldsymbol{A}\mathbf{b}, \boldsymbol{A}^2\mathbf{b}, \cdots, \boldsymbol{A}^{k-1}\mathbf{b}\}$
  - That minimizes $\|\boldsymbol{A}\mathbf{x}^{(k)} - \mathbf{b}\|_2$
- Preconditioning $\boldsymbol{A}\boldsymbol{P}\mathbf{y} = \mathbf{b}, \quad \mathbf{x} = \boldsymbol{P}\mathbf{y}$
- Incomplete LU factorization; fill level p

Solution Scheme — GMRES

- Generalized minimal residual method (GMRES)
  - Finds $\mathbf{x}^{(k)} \in \mathrm{Span}\{\mathbf{b}, \boldsymbol{A}\mathbf{b}, \boldsymbol{A}^2\mathbf{b}, \cdots, \boldsymbol{A}^{k-1}\mathbf{b}\}$
  - That minimizes $\|\boldsymbol{A}\mathbf{x}^{(k)} - \mathbf{b}\|_2$
- Preconditioning $\quad \boldsymbol{A}\boldsymbol{P}\mathbf{y} = \mathbf{b}, \quad \mathbf{x} = \boldsymbol{P}\mathbf{y}$
- Incomplete LU factorization; fill level p
  - $\boldsymbol{A}^* \approx \tilde{\boldsymbol{L}}\tilde{\boldsymbol{U}}$

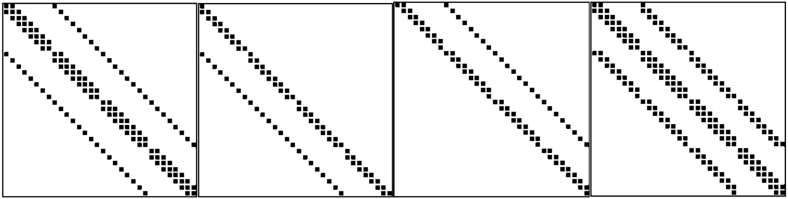

$\boldsymbol{A}$ $\quad$ $\tilde{\boldsymbol{L}}(0)$ $\quad$ $\tilde{\boldsymbol{U}}(0)$ $\quad$ $\tilde{\boldsymbol{L}}\tilde{\boldsymbol{U}}(0)$

Solution Scheme — GMRES

- Generalized minimal residual method (GMRES)
  - Finds $\mathbf{x}^{(k)} \in \text{Span}\{\mathbf{b}, \boldsymbol{A}\mathbf{b}, \boldsymbol{A}^2\mathbf{b}, \cdots, \boldsymbol{A}^{k-1}\mathbf{b}\}$
  - That minimizes $\|\boldsymbol{A}\mathbf{x}^{(k)} - \mathbf{b}\|_2$
- Preconditioning $\quad \boldsymbol{A}\boldsymbol{P}\mathbf{y} = \mathbf{b}, \quad \mathbf{x} = \boldsymbol{P}\mathbf{y}$
- Incomplete LU factorization; fill level p
  - $\boldsymbol{A}^* \approx \tilde{\boldsymbol{L}}\tilde{\boldsymbol{U}}$

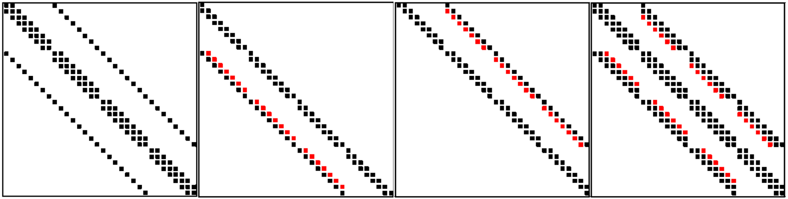

$\boldsymbol{A}$ $\quad$ $\tilde{\boldsymbol{L}}(1)$ $\quad$ $\tilde{\boldsymbol{U}}(1)$ $\quad$ $\tilde{\boldsymbol{L}}\tilde{\boldsymbol{U}}(1)$

Solution Scheme — GMRES

- Generalized minimal residual method (GMRES)
  - Finds $\mathbf{x}^{(k)} \in \mathrm{Span}\{\mathbf{b}, \boldsymbol{A}\mathbf{b}, \boldsymbol{A}^2\mathbf{b}, \cdots, \boldsymbol{A}^{k-1}\mathbf{b}\}$
  - That minimizes $\|\boldsymbol{A}\mathbf{x}^{(k)} - \mathbf{b}\|_2$
- Preconditioning $\quad \boldsymbol{A}\boldsymbol{P}\mathbf{y} = \mathbf{b}, \quad \mathbf{x} = \boldsymbol{P}\mathbf{y}$
- Incomplete LU factorization; fill level p
  - $\boldsymbol{A}^* \approx \tilde{\boldsymbol{L}}\tilde{\boldsymbol{U}}$
  - $\boldsymbol{P} = (\tilde{\boldsymbol{L}}\tilde{\boldsymbol{U}})^{-1}$ (to find $\mathbf{v} = \boldsymbol{P}\mathbf{z}$, solve $(\tilde{\boldsymbol{L}}\tilde{\boldsymbol{U}})\mathbf{v} = \mathbf{z}$)

Solution Scheme — GMRES

- Generalized minimal residual method (GMRES)
  - Finds $\mathbf{x}^{(k)} \in \text{Span}\{\mathbf{b}, \boldsymbol{A}\mathbf{b}, \boldsymbol{A}^2\mathbf{b}, \cdots, \boldsymbol{A}^{k-1}\mathbf{b}\}$
  - That minimizes $\|\boldsymbol{A}\mathbf{x}^{(k)} - \mathbf{b}\|_2$
- Preconditioning $\quad \boldsymbol{A}\boldsymbol{P}\mathbf{y} = \mathbf{b}, \quad \mathbf{x} = \boldsymbol{P}\mathbf{y}$
- Incomplete LU factorization; fill level p
  - $\boldsymbol{A}^* \approx \tilde{\boldsymbol{L}}\tilde{\boldsymbol{U}}$
  - $\boldsymbol{P} = (\tilde{\boldsymbol{L}}\tilde{\boldsymbol{U}})^{-1}$ (to find $\mathbf{v} = \boldsymbol{P}\mathbf{z}$, solve $(\tilde{\boldsymbol{L}}\tilde{\boldsymbol{U}})\mathbf{v} = \mathbf{z}$)
  - Reordering

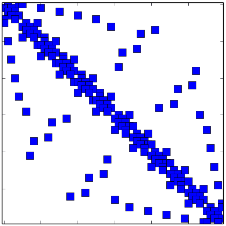

$\boldsymbol{A}$

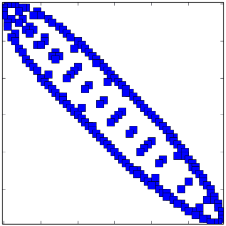

Reordered $\boldsymbol{A}$

Solution Scheme — Preconditioning

- HO-ILUp (Jalali and Ollivier-Gooch, 2017)

Solution Scheme — Preconditioning

- HO-ILUp (Jalali and Ollivier-Gooch, 2017)
  - $\boldsymbol{A} \simeq (\tilde{\boldsymbol{L}}\tilde{\boldsymbol{U}})$ (fill level $p \geq 3$)

Solution Scheme — Preconditioning

- HO-ILUp (Jalali and Ollivier-Gooch, 2017)
  - $\boldsymbol{A} \simeq (\tilde{\boldsymbol{L}}\tilde{\boldsymbol{U}})$ (fill level $p \geq 3$)
  - Memory consuming

Solution Scheme — Preconditioning

- HO-ILUp (Jalali and Ollivier-Gooch, 2017)
  - $\boldsymbol{A} \simeq (\tilde{\boldsymbol{L}}\tilde{\boldsymbol{U}})$ (fill level $p \geq 3$)
  - Memory consuming
- LO-ILUp: (Nejat and Ollivier-Gooch, 2008; Wong and Zingg, 2008)

Solution Scheme — Preconditioning

- HO-ILUp (Jalali and Ollivier-Gooch, 2017)
  - $\boldsymbol{A} \simeq (\tilde{\boldsymbol{L}}\tilde{\boldsymbol{U}})$ (fill level $p \geq 3$)
  - Memory consuming
- LO-ILUp: (Nejat and Ollivier-Gooch, 2008; Wong and Zingg, 2008)
  - $\boldsymbol{A}^{*} \simeq (\tilde{\boldsymbol{L}}\tilde{\boldsymbol{U}})$

Solution Scheme — Preconditioning

- HO-ILUp (Jalali and Ollivier-Gooch, 2017)
  - $\boldsymbol{A} \simeq (\tilde{\boldsymbol{L}}\tilde{\boldsymbol{U}})$ (fill level $p \geq 3$)
  - Memory consuming
- LO-ILUp: (Nejat and Ollivier-Gooch, 2008; Wong and Zingg, 2008)
  - $\boldsymbol{A}^* \simeq (\tilde{\boldsymbol{L}}\tilde{\boldsymbol{U}})$
  - $\boldsymbol{A}^*$ is $k = 0$ LHS matrix

Solution Scheme — Preconditioning

- HO-ILUp (Jalali and Ollivier-Gooch, 2017)
  - $\boldsymbol{A} \simeq (\tilde{\boldsymbol{L}}\tilde{\boldsymbol{U}})$ (fill level $p \geq 3$)
  - Memory consuming
- LO-ILUp: (Nejat and Ollivier-Gooch, 2008; Wong and Zingg, 2008)
  - $\boldsymbol{A}^* \simeq (\tilde{\boldsymbol{L}}\tilde{\boldsymbol{U}})$
  - $\boldsymbol{A}^*$ is $k = 0$ LHS matrix
  - Can be insufficient for $k = 3$

Solution Scheme — Preconditioning

- HO-ILUp (Jalali and Ollivier-Gooch, 2017)
  - $\boldsymbol{A} \simeq (\tilde{\boldsymbol{L}}\tilde{\boldsymbol{U}})$ (fill level $p \geq 3$)
  - Memory consuming
- LO-ILUp: (Nejat and Ollivier-Gooch, 2008; Wong and Zingg, 2008)
  - $\boldsymbol{A}^* \simeq (\tilde{\boldsymbol{L}}\tilde{\boldsymbol{U}})$
  - $\boldsymbol{A}^*$ is $k = 0$ LHS matrix
  - Can be insufficient for $k = 3$
- GMRES-LO-ILUp: (this thesis)

Solution Scheme — Preconditioning

- HO-ILUp (Jalali and Ollivier-Gooch, 2017)
  - $\boldsymbol{A} \simeq (\tilde{\boldsymbol{L}}\tilde{\boldsymbol{U}})$ (fill level $p \geq 3$)
  - Memory consuming
- LO-ILUp: (Nejat and Ollivier-Gooch, 2008; Wong and Zingg, 2008)
  - $\boldsymbol{A}^* \simeq (\tilde{\boldsymbol{L}}\tilde{\boldsymbol{U}})$
  - $\boldsymbol{A}^*$ is $k = 0$ LHS matrix
  - Can be insufficient for $k = 3$
- GMRES-LO-ILUp: (this thesis)
  - Imitates $\boldsymbol{P}(.) = (A^*)^{-1}(.)$

Solution Scheme — Preconditioning

- HO-ILUp (Jalali and Ollivier-Gooch, 2017)
  - $\boldsymbol{A} \simeq (\tilde{\boldsymbol{L}}\tilde{\boldsymbol{U}})$ (fill level $p \geq 3$)
  - Memory consuming
- LO-ILUp: (Nejat and Ollivier-Gooch, 2008; Wong and Zingg, 2008)
  - $\boldsymbol{A}^* \simeq (\tilde{\boldsymbol{L}}\tilde{\boldsymbol{U}})$
  - $\boldsymbol{A}^*$ is $k = 0$ LHS matrix
  - Can be insufficient for $k = 3$
- GMRES-LO-ILUp: (this thesis)
  - Imitates $\boldsymbol{P}(.) = (A^*)^{-1}(.)$
  - Solve $(A^*)\,\{\boldsymbol{P}(.)\} = (.)$ using ILU preconditioned GMRES

Solution Scheme — Preconditioning

- HO-ILUp (Jalali and Ollivier-Gooch, 2017)
  - $\boldsymbol{A} \simeq (\tilde{\boldsymbol{L}}\tilde{\boldsymbol{U}})$ (fill level $p \geq 3$)
  - Memory consuming
- LO-ILUp: (Nejat and Ollivier-Gooch, 2008; Wong and Zingg, 2008)
  - $\boldsymbol{A}^* \simeq (\tilde{\boldsymbol{L}}\tilde{\boldsymbol{U}})$
  - $\boldsymbol{A}^*$ is $k = 0$ LHS matrix
  - Can be insufficient for $k = 3$
- GMRES-LO-ILUp: (this thesis)
  - Imitates $\boldsymbol{P}(.) = (A^*)^{-1}(.)$
  - Solve $(A^*)\,\{\boldsymbol{P}(.)\} = (.)$ using ILU preconditioned GMRES
- ILU reordering

Solution Scheme — Preconditioning

- HO-ILUp (Jalali and Ollivier-Gooch, 2017)
  - $\boldsymbol{A} \simeq (\tilde{\boldsymbol{L}}\tilde{\boldsymbol{U}})$ (fill level $p \geq 3$)
  - Memory consuming
- LO-ILUp: (Nejat and Ollivier-Gooch, 2008; Wong and Zingg, 2008)
  - $\boldsymbol{A}^* \simeq (\tilde{\boldsymbol{L}}\tilde{\boldsymbol{U}})$
  - $\boldsymbol{A}^*$ is $k = 0$ LHS matrix
  - Can be insufficient for $k = 3$
- GMRES-LO-ILUp: (this thesis)
  - Imitates $\boldsymbol{P}(.) = (A^*)^{-1}(.)$
  - Solve $(A^*)\{\boldsymbol{P}(.)\} = (.)$ using ILU preconditioned GMRES
- ILU reordering
  - RCM (minimizes fill of $\boldsymbol{A}^*$)

Solution Scheme — Preconditioning

- HO-ILUp (Jalali and Ollivier-Gooch, 2017)
  - $\boldsymbol{A} \simeq (\tilde{\boldsymbol{L}}\tilde{\boldsymbol{U}})$ (fill level $p \geq 3$)
  - Memory consuming
- LO-ILUp: (Nejat and Ollivier-Gooch, 2008; Wong and Zingg, 2008)
  - $\boldsymbol{A}^* \simeq (\tilde{\boldsymbol{L}}\tilde{\boldsymbol{U}})$
  - $\boldsymbol{A}^*$ is $k = 0$ LHS matrix
  - Can be insufficient for $k = 3$
- GMRES-LO-ILUp: (this thesis)
  - Imitates $\boldsymbol{P}(.) = (A^*)^{-1}(.)$
  - Solve $(A^*)\{\boldsymbol{P}(.)\} = (.)$ using ILU preconditioned GMRES
- ILU reordering
  - RCM (minimizes fill of $\boldsymbol{A}^*$)
  - QMD (minimizes fill of $\tilde{\boldsymbol{L}}\tilde{\boldsymbol{U}}$)

Solution Scheme — Preconditioning

- HO-ILUp (Jalali and Ollivier-Gooch, 2017)
  - $\boldsymbol{A} \simeq (\tilde{\boldsymbol{L}}\tilde{\boldsymbol{U}})$ (fill level $p \geq 3$)
  - Memory consuming
- LO-ILUp: (Nejat and Ollivier-Gooch, 2008; Wong and Zingg, 2008)
  - $\boldsymbol{A}^* \simeq (\tilde{\boldsymbol{L}}\tilde{\boldsymbol{U}})$
  - $\boldsymbol{A}^*$ is $k = 0$ LHS matrix
  - Can be insufficient for $k = 3$
- GMRES-LO-ILUp: (this thesis)
  - Imitates $\boldsymbol{P}(.) = (A^*)^{-1}(.)$
  - Solve $(A^*)\{\boldsymbol{P}(.)\} = (.)$ using ILU preconditioned GMRES
- ILU reordering
  - RCM (minimizes fill of $\boldsymbol{A}^*$)
  - QMD (minimizes fill of $\tilde{\boldsymbol{L}}\tilde{\boldsymbol{U}}$)
  - Lines of strong coupling between unknowns (this thesis)

Solution Scheme — Lines of Strong Unknown Coupling

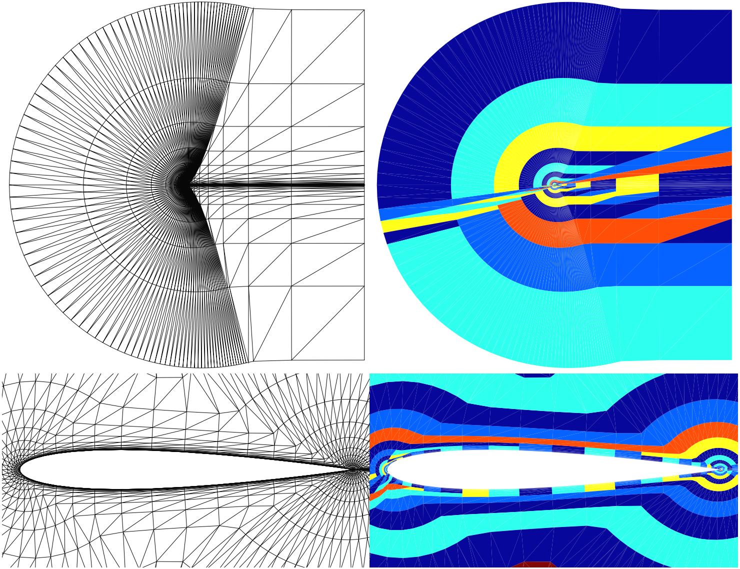

Solution Scheme — Results

- $k = 3$
- 2-D turbulent flow over NACA 0012
- $Re = 6 \times 10^6$, $Ma = 0.15$, $\alpha = 10^\circ$
- Mixed mesh with $N_{\mathrm{CV}} = 100\mathrm{K}$ and $N_{\mathrm{CV}} = 25\mathrm{K}$

Case name	Preconditioning method	Reordering algorithm	Used in higher-order FV
A	HO-ILU3	QMD	(Jalali and Ollivier-Gooch, 2017)
B	LO-ILU0	RCM	(Nejat and Ollivier-Gooch, 2008)
C	LO-ILU0	lines	This thesis
D	GMRES-LO-ILU0	RCM	This thesis
E	GMRES-LO-ILU0	lines	This thesis

Solution Scheme — Results

Comparison of residual histories

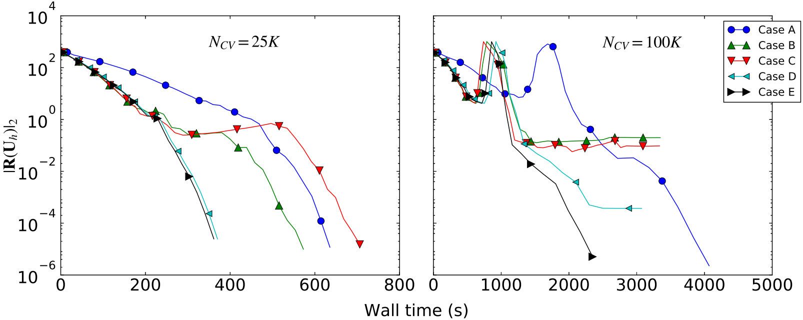

Inviscid Flow Around Sphere

- $Ma = 0.38$
- $N_{\mathrm{CV}} = 64\mathrm{K}, 322\mathrm{K}, 1\mathrm{M}$

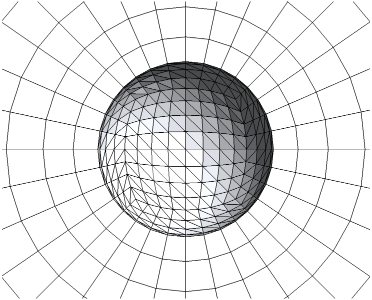

Inviscid Flow Around Sphere — Entropy Norm

Subsonic flow $\longrightarrow \|S - S_\infty\|_2 = 0$

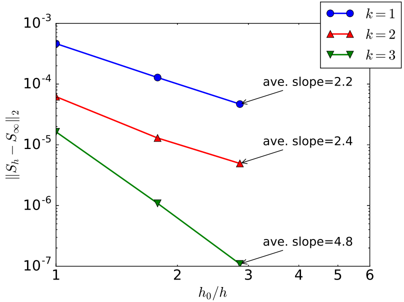

Turbulent Flow Over a Flat Plate

- $Re = 5 \times 10^6$
- $Ma = 0.2$
- Nested meshes: $60 \times 34 \times 7$, $120 \times 68 \times 14$, and $240 \times 136 \times 28$

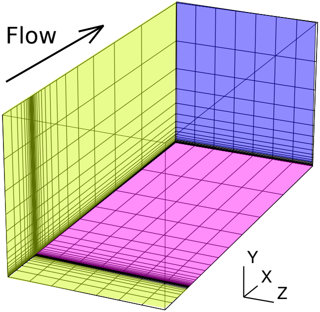

Adiabatic wall.
Symmetry
Inflow/outflow

Turbulent Flow Over a Flat Plate — Verification

Distribution of the turbulence working variable on the plane $x_3 = 0.5$

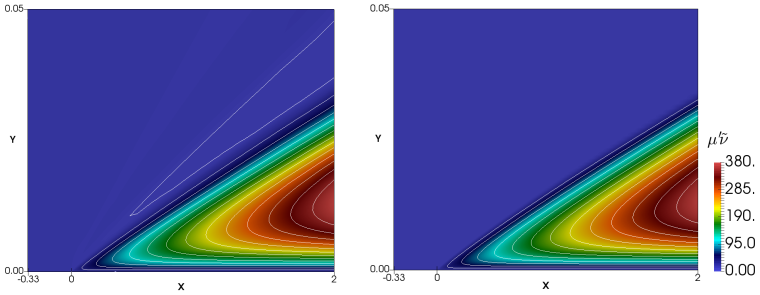

$k = 3$
$240 \times 136 \times 28$

NASA TMR
544×384

Turbulent Flow Over a Flat Plate — Verification

Eddy viscosity on the line $(x_1 = 0.97) \wedge (x_3 = 0.5)$

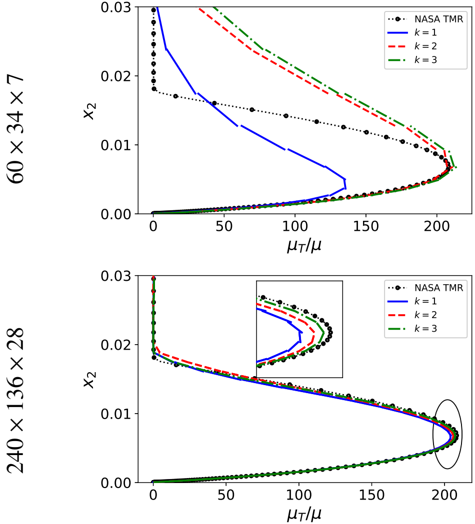

Turbulent Flow Over an Extruded NACA 0012

- Extrusion length = 1 in x_3 direction
- $Re = 6 \times 10^6$, $Ma = 0.15$, $\alpha = 10°$, $\psi = 0$
- Hex mesh with $N_{CV} = 100K$ and mixed mesh with $N_{CV} = 176K$

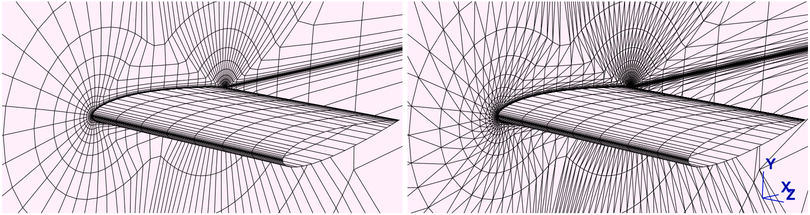

Extruded NACA 0012 — Convergence

- Norm of the residual vector per PTC iteration
- Order ramping
- Convergence only slightly affected by mesh type or k

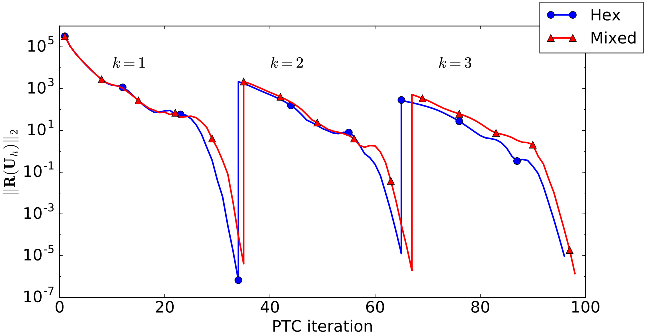

Extruded NACA 0012 — Verification

Surface pressure coefficient at $x_3 = 0.5$

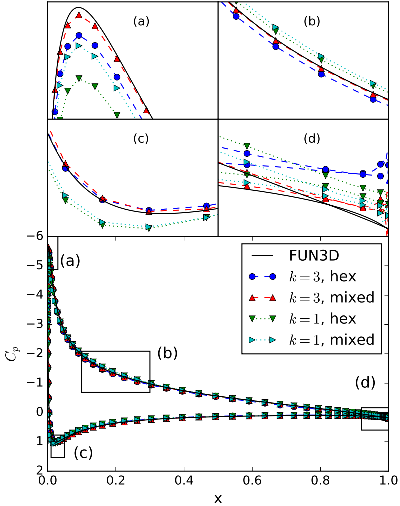

Summary

- Derived the k-exact finite volume formulation of the RANS + negative S-A equations in 3-D.

Summary

- Derived the k-exact finite volume formulation of the RANS + negative S-A equations in 3-D.
- Developed a 3-D linear elasticity solver to prevent mesh tangling.

Summary

- Derived the k-exact finite volume formulation of the RANS + negative S-A equations in 3-D.
- Developed a 3-D linear elasticity solver to prevent mesh tangling.
- Designed an efficient solution scheme.

Summary

- Derived the k-exact finite volume formulation of the RANS + negative S-A equations in 3-D.
- Developed a 3-D linear elasticity solver to prevent mesh tangling.
- Designed an efficient solution scheme.
  - Lines of strong coupling between unknowns.

Summary

- Derived the k-exact finite volume formulation of the RANS + negative S-A equations in 3-D.
- Developed a 3-D linear elasticity solver to prevent mesh tangling.
- Designed an efficient solution scheme.
  - Lines of strong coupling between unknowns.
  - Inner GMRES iterations based on the $k = 0$ scheme.

Summary

- Derived the k-exact finite volume formulation of the RANS + negative S-A equations in 3-D.
- Developed a 3-D linear elasticity solver to prevent mesh tangling.
- Designed an efficient solution scheme.
    - Lines of strong coupling between unknowns.
    - Inner GMRES iterations based on the $k = 0$ scheme.
- Verified the developed solver for benchmark problems.

References I

Bassi, F. and Rebay, S. (1997). High-order accurate discontinuous finite element solution of the 2D Euler equations. *Journal of Computational Physics*, 138(2):251–285.

Haider, F., Brenner, P., Courbet, B., and Croisille, J.-P. (2014). Parallel implementation of k-exact finite volume reconstruction on unstructured grids. In *High-Order Nonlinear Numerical Schemes for Evolutionary PDEs*, pages 59–75. Springer.

Haider, F., Croisille, J.-P., and Courbet, B. (2009). Stability analysis of the cell centered finite-volume Muscl method on unstructured grids. *Numerische Mathematik*, 113(4):555–600.

Jalali, A. and Ollivier-Gooch, C. (2017). Higher-order unstructured finite volume RANS solution of turbulent compressible flows. *Computers and Fluids*, 143:32–47.

Li, W. (2014). *Efficient Implementation of High-Order Accurate Numerical Methods on Unstructured Grids*. Springer.

Michalak, C. and Ollivier-Gooch, C. (2009). Accuracy preserving limiter for the high-order accurate solution of the Euler equations. *Journal of Computational Physics*, 228(23):8693–8711.

Nejat, A. and Ollivier-Gooch, C. (2008). Effect of discretization order on preconditioning and convergence of a high-order unstructured Newton-GMRES solver for the Euler equations. *Journal of Computational Physics*, 227(4):2366–2386.

References II

Ollivier-Gooch, C. F. and Van Altena, M. (2002). A high-order accurate unstructured mesh finite-volume scheme for the advection-diffusion equation. *Journal of Computational Physics*, 181(2):729–752.

Wong, P. and Zingg, D. W. (2008). Three-dimensional aerodynamic computations on unstructured grids using a Newton–Krylov approach. *Computers and Fluids*, 37(2):107–120.

FV vs DG

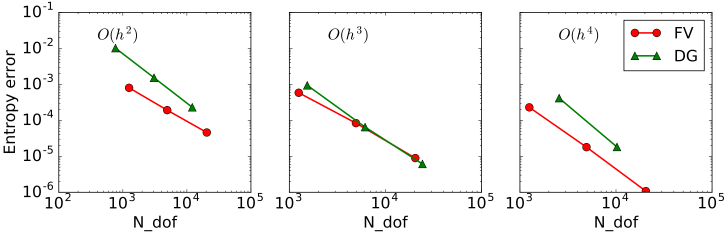

Inviscid flow around a circle (Bassi and Rebay, 1997)

Common Goal

- Given a PDE $\mathcal{L}\mathbf{u}(\mathbf{x}) = 0$
- Find a discrete solution $\mathbf{u}_h(\mathbf{x}; \mathbf{U}_h)$
- Such that the discretization error $\mathbf{e}_h = \mathbf{u}_h - \mathbf{u}$
- Has an asymptotic behavior $\|\mathbf{e}_h\| = O(h^p)$

The method is said to be pth-order accurate.

Traditional methods are second-order accurate.

Higher-Order Methods — Advantages

Reduction of computational costs.

- When modeling errors are dominant:
  - Limited level of reduction in discretization error is of interest.
  - *hp*-adaptive methods.
- When numerical errors are dominant:
  - E.g., complicated full-body aircraft geometries.
  - E.g., advanced turbulence modeling schemes.
  - More accurate solution are valuable (1% better accuracy in finding drag).
  - Accurate solutions can be obtained on coarser meshes.
- Unstructured finite volume methods
  - Complex geometries
  - Fewer number of degrees of freedom.
  - Easier integration into commercial solvers.

K-exact reconstruction — Continued

- Satisfy conservation of the mean.
- Predict the average values of *Stencil*(τ) closely.

$$
\begin{aligned}
\underset{a_\tau^1 \ldots a_\tau^{N_{\mathrm{rec}}}}{\text{minimize}} \quad & \sum_{\sigma \in Stencil(\tau)} \left(\frac{1}{\Omega_\sigma} \int_\sigma u_{h,\tau}(\mathbf{x}) d\Omega - U_{h,\sigma} \right)^2 \\
\text{subject to} \quad & \frac{1}{\Omega_\tau} \int_\tau u_h(\mathbf{x}) d\Omega = U_{h,\tau}
\end{aligned}
$$

K-exact reconstruction — Continued

- Satisfy conservation of the mean.
- Predict the average values of *Stencil*(τ) closely.

$$I^i_{\tau\sigma} = \int_\sigma \phi^i_\tau(\mathbf{x})d\Omega \qquad \sigma \in \mathit{Stencil}(\tau) \cup \{\tau\}$$

$$\left[\begin{array}{ccc} I^1_{\tau\tau} & \dots & I^{N_\text{rec}}_{\tau\tau} \\ \hline I^1_{\tau\sigma_1} & \dots & I^{N_\text{rec}}_{\tau\sigma_1} \\ \vdots & \ddots & \vdots \\ I^1_{\tau\sigma_{\text{NS}(\tau)}} & \dots & I^{N_\text{rec}}_{\tau\sigma_{\text{NS}(\tau)}} \end{array}\right] \begin{bmatrix} a^1_\tau \\ \vdots \\ a^{N_\text{rec}}_\tau \end{bmatrix} = \left[\begin{array}{c} U_{h,\tau} \\ \hline U_{h,\sigma_1} \\ \vdots \\ U_{h,\sigma_{\text{NS}(\tau)}} \end{array}\right]$$

K-exact reconstruction — Continued

- Satisfy conservation of the mean.
- Predict the average values of *Stencil*(τ) closely.

$$\begin{bmatrix} a_\tau^1 \\ \vdots \\ a_\tau^{N_{\text{rec}}} \end{bmatrix} = \boldsymbol{A}_\tau^\dagger \begin{bmatrix} U_{h,\tau} \\ U_{h,\sigma_1} \\ \vdots \\ U_{h,\sigma_{\text{NS}(\tau)}} \end{bmatrix}$$

Reconstruction Optimization Problem

- $Ax = b$ subject to $Bx = 0$
- Change of variables $x = By$ where the columns of B are the null space of A.
- $Ax = 0$ reduces to $(AB = C)y = 0$ which is always satisfied.
- Solve the unconstrained problem $Cy = b$, i.e., $y = C^{\dagger}b$
  - QR (Householder or Gram-schmidt): $C = Q_1R_1$, $C^{\dagger} = R_1^{-1}Q^T$
  - SVD (most stable): $C = U\Sigma V^T$, $C^{\dagger} = W^T\Sigma^{-1}U$
  - Normal equations: $C^{\dagger} = (CC^T)^{-1}C^T$
- Finally, $x = By$.

Numerical Flux Functions

Inviscid Flux — Roe's Flux Function

$\mathcal{F}(\mathbf{u}_h^+, \mathbf{u}_h^-)$ = approximate solution for $\boldsymbol{F}(s = 0)\mathbf{n}$ in

$$\begin{cases} \frac{\partial \mathbf{u}}{\partial t} + \frac{\partial \boldsymbol{F}(\mathbf{u})\mathbf{n}}{\partial s} = 0 \\ \mathbf{u}(s < 0, t = 0) = u_h^- \\ \mathbf{u}(s > 0, t = 0) = u_h^+ \end{cases}$$

Inviscid Flux — Averaging with Damping

$$\mathcal{Q}(\mathbf{u}_h^+, \nabla\mathbf{u}_h^+, \mathbf{u}_h^-, \nabla\mathbf{u}_h^-) = \boldsymbol{Q}(\mathbf{u}_h^*, \nabla\mathbf{u}_h^*)\mathbf{n},$$

where $\mathbf{u}_h^* = \frac{1}{2}\left(\mathbf{u}_h^+ + \mathbf{u}_h^-\right),$

and $\nabla\mathbf{u}_h^* = \frac{1}{2}\left(\nabla\mathbf{u}_h^+ + \nabla\mathbf{u}_h^-\right) + \eta\left(\frac{\mathbf{u}_h^+ - \mathbf{u}_h^-}{\|\mathbf{x}_{\tau+} - \mathbf{x}_{\tau-}\|_2}\right)\mathbf{n}$

Parallel Scaling

Strong Scaling Test

- Solving the same problem with different number of processors
- Inviscid flow, sphere: $N_{\mathrm{CV}} = 322\mathrm{K}$ and $k = 3$
- Turbulent flow, flat plate: $128 \times 68 \times 14$ mesh and $k = 3$

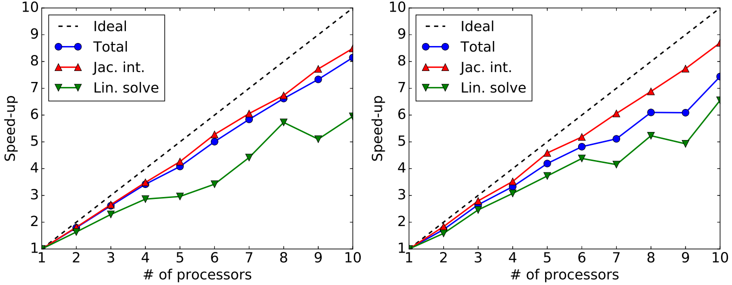

Sphere Flat plate

Nondimensionalization – Flow Variables

Reference values:

$$\rho^* \sim \rho_\infty \quad \mathbf{v}^* \sim c_\infty \quad T^* \sim \frac{c_\infty}{\gamma R} \quad P^* \sim \rho_\infty c_\infty^2$$
$$t^* \sim \frac{L}{c_\infty} \quad \mu^* \sim \mu_\infty \quad \mu_T^* \sim \mu_\infty \quad \nu_T^* \sim \frac{\mu_\infty}{\rho_\infty}$$
$$\tilde{\nu}^* \sim \mu' \quad \boldsymbol{\tau} \sim \frac{\mu_\infty c_\infty}{L} \quad d \sim L$$

Pressure and temperature:

$$c^* = \sqrt{\frac{\gamma P^*}{\rho^*}} \quad \Rightarrow \quad c = \sqrt{\frac{\gamma P}{\rho}}$$

$$P^* = \rho^* R T^* \quad \Rightarrow \quad P = \frac{\rho T}{\gamma}$$

$$E^* = \rho \frac{R(\gamma-1)}{\gamma} T + \frac{1}{2}(\mathbf{v}^* \cdot \mathbf{v}^*) \Rightarrow P = (\gamma - 1)\left(E - \frac{1}{2}\rho(\mathbf{v} \cdot \mathbf{v})\right)$$

Dimensionless numbers:

$$Ma = \frac{v_\infty}{c_\infty} \quad Re = \frac{\rho_\infty v_\infty L}{\mu_\infty} \quad Pr = \frac{c_p \mu}{k}$$

Nondimensionalization — Lift and Drag

$$\text{Pressure Force} \sim \rho_\infty c_\infty^2 L^2$$

$$\text{Viscous Force} \sim \mu_\infty c_\infty L^2$$

$$C_D = \frac{D^*}{(1/2)\rho_\infty v_\infty^2 A} \;\Rightarrow\; C_D = \frac{D}{(1/2)\, Ma^2 (A/L^2)}$$

$$C_{Dv} = \frac{D^*}{(1/2)\rho_\infty v_\infty^2 A} \Rightarrow C_{Dv} = \frac{D}{(1/2)\, Ma\, Re (A/L^2)}$$

$$C_f = \frac{\mathbf{m}^T \boldsymbol{\tau}^* \mathbf{n}}{(1/2)\rho^* v_\infty^2 A} \;\Rightarrow C_f = \frac{\mathbf{m}^T \boldsymbol{\tau} \mathbf{n}}{(1/2)\rho\, Ma\, Re (A/L^2)}$$

Nondimensionalization — Sutherland's Law

$$\frac{\mu^*}{\mu_{ref}} = \left(\frac{T^*}{T_{ref}}\right)^{3/2} \frac{1 + (S^*/T_{ref})}{(T^*/T_{ref}) + (S^*/T_{ref})}$$

$$\mu = T\frac{\mu_\infty}{\mu_{ref}}\frac{(T_{ref}/T_\infty) + S}{T + S}$$

$$S = 110.4K \quad T_{ref} = 273.15K \quad \mu_{ref} = 1.716 \times 10^{-5}$$

Nondimensionalization — Flux Matrices

$$\boldsymbol{F}^* = \begin{bmatrix} \rho^* \mathbf{v}^{*T} \\ \rho^* \mathbf{v}^* \mathbf{v}^{*T} + P^* \boldsymbol{I} \\ (E^* + P^*)\mathbf{v}^{*T} \\ \tilde{\nu}^* \rho^* \mathbf{v}^{*T} \end{bmatrix} \quad \boldsymbol{Q}^* = \begin{bmatrix} 0 \\ \boldsymbol{\tau}^* \\ (E^* + P^*)\boldsymbol{\tau}^* \mathbf{v}^* + \frac{R\gamma}{\gamma-1}\left(\frac{\mu^*}{Pr} + \frac{\mu_T^*}{Pr_T}\right)\nabla T^* \\ -\frac{1}{\sigma}(\mu^* + \mu_T^*)\nabla\tilde{\nu}^* \end{bmatrix}$$

$$\boldsymbol{F} = \begin{bmatrix} \rho \mathbf{v}^{T} \\ \rho \mathbf{v} \mathbf{v}^{T} + P \boldsymbol{I} \\ (E + P)\mathbf{v}^{T} \\ \tilde{\nu} \rho \mathbf{v}^{T} \end{bmatrix} \quad \boldsymbol{Q} = \begin{bmatrix} 0 \\ \frac{Ma}{Re}\boldsymbol{\tau} \\ (E + P)\boldsymbol{\tau} \mathbf{v} + \frac{1}{\gamma-1}\left(\frac{\mu}{Pr} + \frac{\mu_T}{Pr_T}\right)\nabla T \\ -\frac{Ma}{Re\,\sigma}(\mu + \mu_T)\nabla\tilde{\nu} \end{bmatrix}$$

Solution Scheme — PTC

- Seeking the steady state solution of:

$$\frac{d\mathbf{U}_h}{dt} + \mathbf{R}(\mathbf{U}_h) = 0$$

- Newton:

$$\frac{\partial \mathbf{R}}{\partial \mathbf{U}_h}\delta\mathbf{U}_h = -\mathbf{R}(\mathbf{U}_h), \quad \mathbf{U}_h \leftarrow \mathbf{U_h} + \delta\mathbf{U_h}$$

- Backward Euler:

$$\frac{\mathbf{U}_h^+ - \mathbf{U}_h}{\Delta t} + \mathbf{R}(\mathbf{U}_h) = 0$$

- Pseudo transient continuation:

$$\left(\frac{\boldsymbol{V}}{\Delta t} + \frac{\partial \mathbf{R}}{\partial \mathbf{U}_h}\right)\delta\mathbf{U}_h = -\mathbf{R}(\mathbf{U}_h)$$

- A linear system must be solved:

$$\boldsymbol{A}\mathbf{x} = \mathbf{b} \quad (*)$$

Solution Scheme — Preconditioning

- GMRES can stall
- Right preconditioning $\boldsymbol{AP}\mathbf{y} = \mathbf{b}, \quad \mathbf{x} = \boldsymbol{P}\mathbf{y}$
- Incomplete LU factorization; fill level p
  - $\boldsymbol{A}^* \approx \tilde{\boldsymbol{L}}\tilde{\boldsymbol{U}}$
  - $P = (\tilde{\boldsymbol{L}}\tilde{\boldsymbol{U}})^{-1}$ (to find $\mathbf{v} = \boldsymbol{P}\mathbf{z}$, solve $(\tilde{\boldsymbol{L}}\tilde{\boldsymbol{U}})\mathbf{v} = \mathbf{z}$)
  - Reordering $\boldsymbol{\sigma A \sigma^T P}\mathbf{y} = \boldsymbol{\sigma}\mathbf{b}$

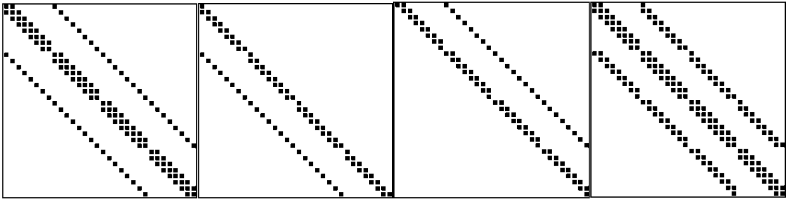

$\boldsymbol{A}$ $\quad \tilde{\boldsymbol{L}}(0)$ $\quad \tilde{\boldsymbol{U}}(0)$ $\quad \tilde{\boldsymbol{L}}\tilde{\boldsymbol{U}}(0)$

Solution Scheme — Preconditioning

- GMRES can stall
- Right preconditioning $\boldsymbol{AP}\mathbf{y} = \mathbf{b}, \quad \mathbf{x} = \boldsymbol{P}\mathbf{y}$
- Incomplete LU factorization; fill level p
  - $A^* \approx \tilde{\boldsymbol{L}}\tilde{\boldsymbol{U}}$
  - $P = (\tilde{\boldsymbol{L}}\tilde{\boldsymbol{U}})^{-1}$ (to find $\mathbf{v} = \boldsymbol{P}\mathbf{z}$, solve $(\tilde{\boldsymbol{L}}\tilde{\boldsymbol{U}})\mathbf{v} = \mathbf{z}$)
  - Reordering $\boldsymbol{\sigma A \sigma^T P}\mathbf{y} = \boldsymbol{\sigma}\mathbf{b}$

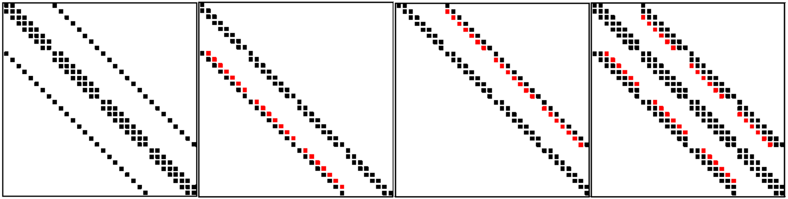

$\boldsymbol{A}$ $\quad\tilde{\boldsymbol{L}}(1)$ $\quad\tilde{\boldsymbol{U}}(1)$ $\quad\tilde{\boldsymbol{L}}\tilde{\boldsymbol{U}}(1)$

Solution Scheme — Preconditioning

- GMRES can stall
- Right preconditioning $\quad \boldsymbol{AP}\mathbf{y} = \mathbf{b}, \quad \mathbf{x} = \boldsymbol{P}\mathbf{y}$
- Incomplete LU factorization; fill level p
  - $A^* \approx \tilde{\boldsymbol{L}}\tilde{\boldsymbol{U}}$
  - $P = (\tilde{\boldsymbol{L}}\tilde{\boldsymbol{U}})^{-1}$ (to find $\mathbf{v} = \boldsymbol{P}\mathbf{z}$, solve $(\tilde{\boldsymbol{L}}\tilde{\boldsymbol{U}})\mathbf{v} = \mathbf{z}$)
  - Reordering $\quad \boldsymbol{\sigma A \sigma^T P}\mathbf{y} = \boldsymbol{\sigma}\mathbf{b}$

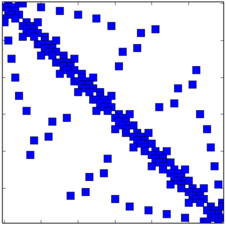

$\boldsymbol{A}$

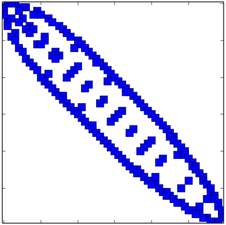

$\boldsymbol{\sigma A \sigma^T}$

Solution Scheme — Lines of Strong Unknown Coupling

- Assign binary weights $W_{\tau\sigma}$.
- Advection-diffusion equation $\nabla \cdot (\mathbf{v}u - \mu_L \nabla u) = 0$.
- $W_{\tau\sigma} = \max\left(\frac{\partial R_\sigma}{\partial u_\tau}, \frac{\partial R_\tau}{\partial u_\sigma}\right)$
- Greedy clustering algorithm
  1. Pick an unmarked control volume τ
  2. Pick the neighbour σ with the highest weight
  3. If σ is marked go to 1.
  4. Add σ to line and mark it.
  5. $\tau = \sigma$, go to 2.

Solution Scheme — Comparison Details

Preconditioner	N-PTC	N-GMRES	Memory(GB)	LST(s)	TST(s)
		$N_{\mathrm{CV}} = 25\mathrm{K}$			
A	37	956	1.4	416	635
B	44	10, 893	0.7	264	572
C	51	13, 692	0.7	328	705
D	34	1, 856	0.7	134	379
E	34	1, 787	0.7	118	361
		$N_{\mathrm{CV}} = 100\mathrm{K}$			
A	39	4, 640	5.9	3, 122	4, 068
B	–	–	2.8	–	–
C	–	–	2.8	–	–
D	–	–	3.2	–	–
E	36	4, 396	3.2	1, 308	2, 348

Poisson's Equation

- $\nabla^2 u = f$
- Manufactured solution
  $u = \sinh(\sin(x_1)) \sinh(\sin(x_2)) \sinh(\sin(x_3))$
- Domain $\Omega = [0 \quad 1]^3$
- Dirichlet boundary conditions

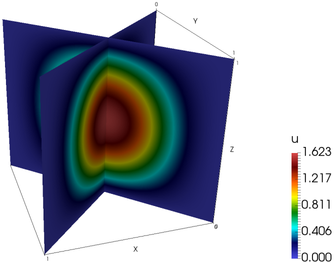

Poisson's Equation — Accuracy Analysis

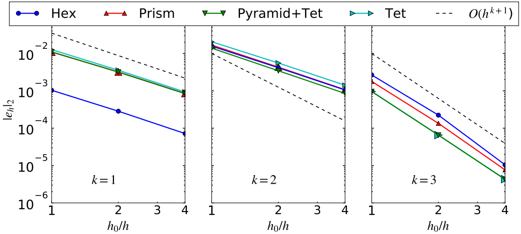

Error versus mesh length scale

Poor performance of $k = 2$ is expected (Ollivier-Gooch and Van Altena, 2002).

Poisson's Equation — Meshes

$$N = 10, 20, 40.$$

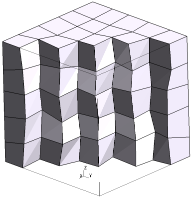

Hexahedra

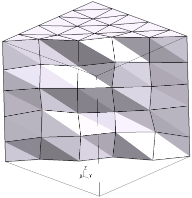

Prisms

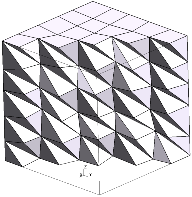

Pyramids+Tetrahedra

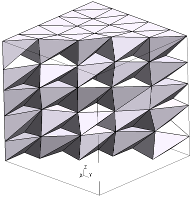

Tetrahedra

Inviscid Flow Around Sphere — Mach Contours

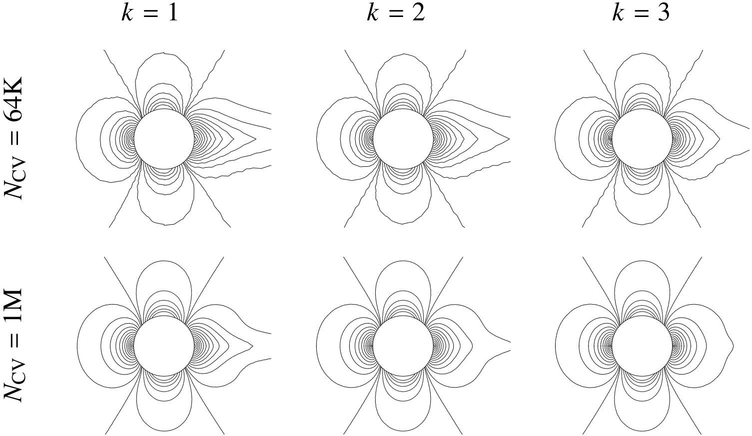

Computed Mach contours on the $x_3 = 0$ symmetry plane for the sphere problem

Sphere — Convergence

- Norm of the residual vector per PTC iteration
- Free-stream state as initial conditions.

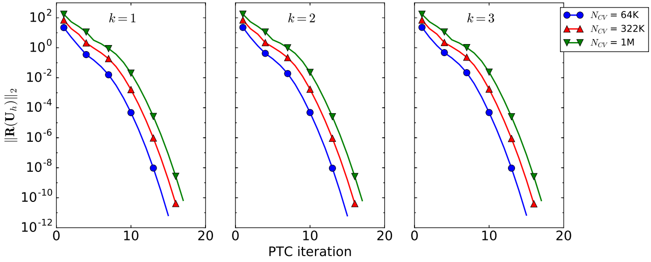

Sphere — Performance

k	N-PTC	N-GMRES	Memory(GB)	LST(s)	TST(s)
			N_{CV} = 64K		
1	15	182	2.94	24	107
2	15	181	3.91	20	112
3	15	255	6.00	31	320
			N_{CV} = 322K		
1	16	207	13.24	134	579
2	16	212	14.05	132	620
3	16	300	28.39	271	1,879
			N_{CV} = 1M		
1	17	275	39.48	486	1,969
2	17	277	45.52	536	2,150
3	17	385	85.78	793	5,904

Flat Plate — Convergence

- Norm of the residual vector per PTC iteration
- Solution of $(k + 1)$-exact scheme is initialized with that of k-exact.

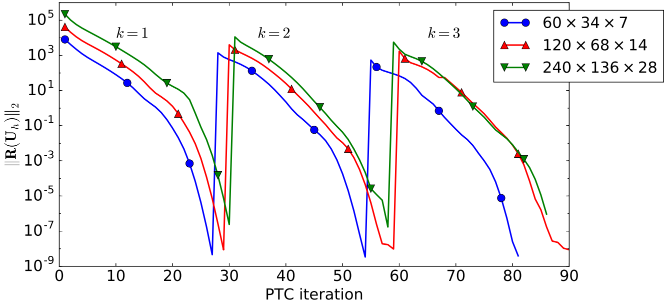

Flat Plate — Drag

Computed value and convergence order of the drag coefficient and the skin friction coefficient at the point $\mathbf{x} = (0.97, 0, 0.5)$

	C_D			C_f		
NASA TMR	0.00286			0.00271		
Mesh \ k	1	2	3	1	2	3
$60 \times 34 \times 7$	0.00396	0.00233	0.00233	0.00350	0.00228	0.00222
$120 \times 68 \times 14$	0.00301	0.00281	0.00285	0.00283	0.00268	0.00271
$240 \times 136 \times 28$	0.00287	0.00286	0.00286	0.00274	0.00273	0.00273
Convergence order	2.8	3.3	5.4	3	3	5.1

Flat Plate — Performance

k	N-PTC	N-GMRES	Memory(GB)	LST(s)	TST(s)
		$60 \times 34 \times 7$ mesh			
1	26	844	0.42	31	55
2	26	1, 009	1.35	42	124
3	26	1, 071	2.10	57	202
		$120 \times 68 \times 14$ mesh			
1	28	1, 436	5.24	510	713
2	29	1, 864	8.30	742	1, 489
3	29	2, 041	14.63	825	2, 124
		$240 \times 136 \times 28$ mesh			
1	29	2, 492	38.77	6, 222	7, 884
2	27	3, 305	60.70	12, 353	18, 137
3	27	2, 906	121.81	23, 141	35, 412

Extruded NACA 0012 — $\tilde{\nu}$

Distribution of the turbulence working variable for the extruded NACA 0012 problem on the $x_3 = 0$ plane, $k = 3$.

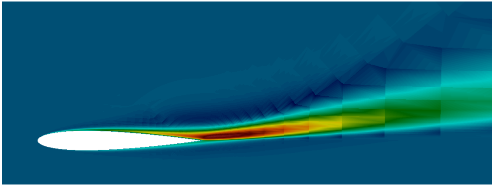

(a) Hexahedral mesh

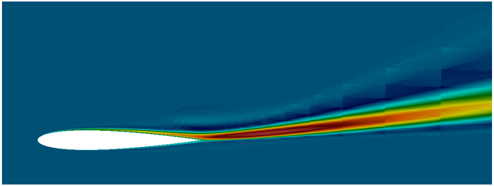

(b) Mixed prismatic-hexahedral mesh

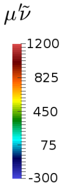

Extruded NACA 0012 — Drag

Computed value and convergence order of the drag coefficient and the skin friction coefficient at the point $\mathbf{x} = (0.97, 0, 0.5)$

k	C_{Dp}	C_{Dv}	C_L
NASA TMR			
–	0.00607	0.00621	1.0910
Hex mesh			
1	0.01703	0.00582	1.0619
2	0.01702	0.00497	1.0507
3	0.00301	0.00472	1.0417
Mixed mesh			
1	0.01129	0.00574	1.0735
2	0.00365	0.00565	1.0776
3	0.00550	0.00536	1.0869

Extruded NACA 0012 — Performance

k	N-PTC	N-GMRES	Memory(GB)	LST(s)	TST(s)
Hex mesh, $N_{\mathrm{CV}} = 100\mathrm{K}$					
1	33	1,154	4.77	317	744
2	31	1,788	6.82	730	2,097
3	31	2,415	12.23	1,057	3,215
Mixed mesh, $N_{\mathrm{CV}} = 176\mathrm{K}$					
1	34	1,132	8.70	458	1,164
2	32	1,769	10.87	800	2,427
3	31	2,185	26.47	1,311	4,666